Geomorphic change detection in Gadria-Strimm and Moscardo catchments, Italy

Report

Guidelines for assessing sediment dynamics in alpine basins and channel reaches

WP4 Basin-scale Sediment Dynamics

Action 4.1: Sediment sources
Action 4.2: Sediment connectivity
Action 4.3: Sediment yields
Action 4.4: Sediment cascades
Action 4.5: Historical analysis of basin responses

ANNEX

Case studies and software tools

Contributors: M. Becht, C. Bel, M. Bertrand, N. Bezac, G. Blasone, F. Brardinoni, M. Cavalli, F. Cazorzi, S. Crema, B. Goldin, F. Haas, T. Heckmann, A. Huber, S. Lallias-Tacon, F. Liébault, L. Marchi, M. Mikoš, Eintrag, O. Passalacqua, H. Piégay, S. Rusjan, R. Scotti, R. Sosio, D. Tiranti, M. Zerbato

May 29th, 2015

www.sedalp.eu

Sediment management in Alpine basins

Table of contents

8 Annex: Case studies

8.1 Geomorphic change detection in Gadria-Strimm and Moscardo catchments, Italy (PP4)

M. Cavalli[1], B. Goldin[1], S. Crema[1], F. Brardinoni[1,2], L. Marchi[1], G. Blasone[3], F. Cazorzi[3]

[1] CNR IRPI, Padova (PP4)

[2] University of Milano-Bicocca

[3] University of Udine

8.1.1 Introduction

Methods devoted to the assessment of geomorphic changes can be used to identify geomorphologically unstable areas, to quantify processes intensity, and to compute sediment budgets. Digital elevation models (DEMs) built from repeated topographic surveys can be used to produce DEM of Difference (DoD) maps whose analysis allows to study morphological changes in slopes and channels from the quantitative (scour and fill changes in volume) and the qualitative (spatial patterns of erosion and deposition) perspectives (Scheidl et al., 2008; Theule et al., 2012; Picco et al., 2013). The activity carried out by CNR IRPI (PP4) in the frame of the SedAlp project focused on the analysis of multi temporal high-resolution Digital Terrain Models (DTMs) derived by Airborne and Terrestrial LiDAR. The aim is to analyse surface changes due to erosion and deposition in a bedload and two debris-flow prone basins in the Eastern Italian Alps (Strimm, Gadria and Moscardo pilot areas). The analysis was carried out at different temporal and spatial scales basically related to the typology of the adopted surveying method. In Gadria and Strimm catchments, where two airborne LiDAR (2005 and 2011) are available, geomorphic changes induced by debris flows and landslides were investigated at catchment scale. DoD results have been then compared with field estimations stored in a historical database. In the Moscardo catchment, Terrestrial Laser Scanner (TLS) has been used to survey three representative areas of the catchment in a small time window (August 2011-October 2012). Results of volumetric budgets of the surveyed sediment source areas derived from DoD analysis have been compared with debris-flow volumes estimated from flow stage measurements at the instrumented channel reach.

8.1.2 Study areas

8.1.2.1 Strimm and Gadria catchments

The Strimm and Gadria catchments are two adjacent basins located in the upper Vinschgau-Venosta valley (Eastern Alps, Italy) (Figure 8-1 and Table 8-1). Gadria and Strimm creeks join at a filter check dam located near the apex of their large alluvial fan (10.9 km²). The combination of steep topography, highly deformed-fractured metamorphic rocks and thick glacio-fluvial deposits, sets the conditions for chronic debris-flow activity within the Gadria channel network (Comiti et al., 2014.). The Strimm is essentially a bedload stream in which debris flows occur only in the steepest parts of the catchment and rarely in a few sectors of the main channel (Cavalli et al., 2013). A monitoring station was installed in 2011 in the Gadria for monitoring debris flows and testing warning procedures (Comiti et al., 2014).

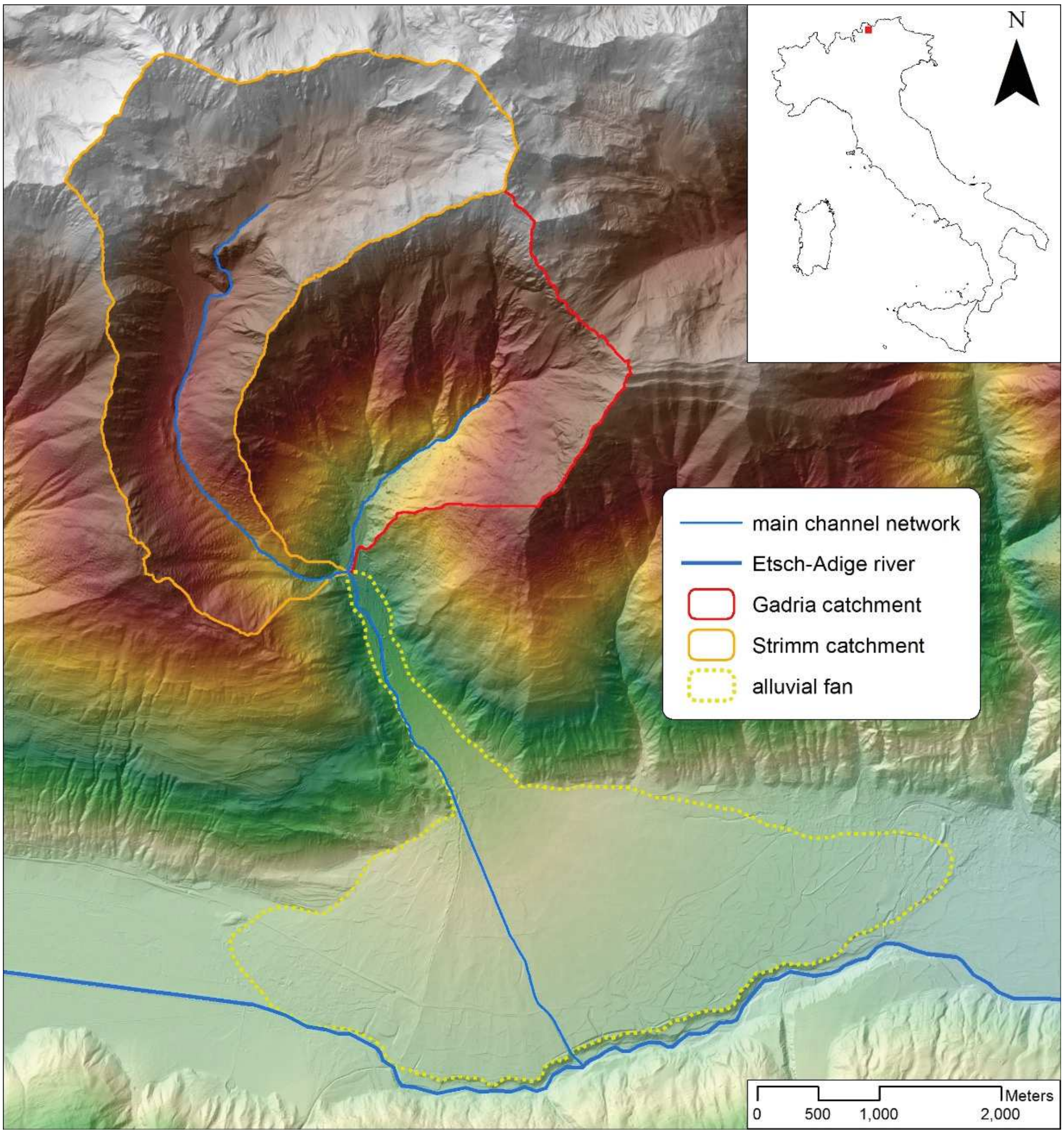

Figure 8-1: Location map of Gadria and Strimm catchments (Comiti et al., 2014)

8.1.2.2 Moscardo torrent

The Moscardo catchment is a debris-flow prone basin located in Friuli Venezia Giulia (Eastern Alps, Italy) (Figure 8-2 and Table 8-1). A debris-flow monitoring system has been in operation in the Moscardo Torrent since 1989 (Marchi et al., 2002). The presence of a deep-seated gravitational deformation at the valley head, the low rock mass quality and its highly shattered state make the steep slopes of the basin prone to rockfalls and shallow slope failures that supply large amounts of debris to the channel. Large sediment source areas are present in the upper part of the basin and along the main channel. Debris-flow initiation points can vary from event to event, being generally located at the head of the main channel.

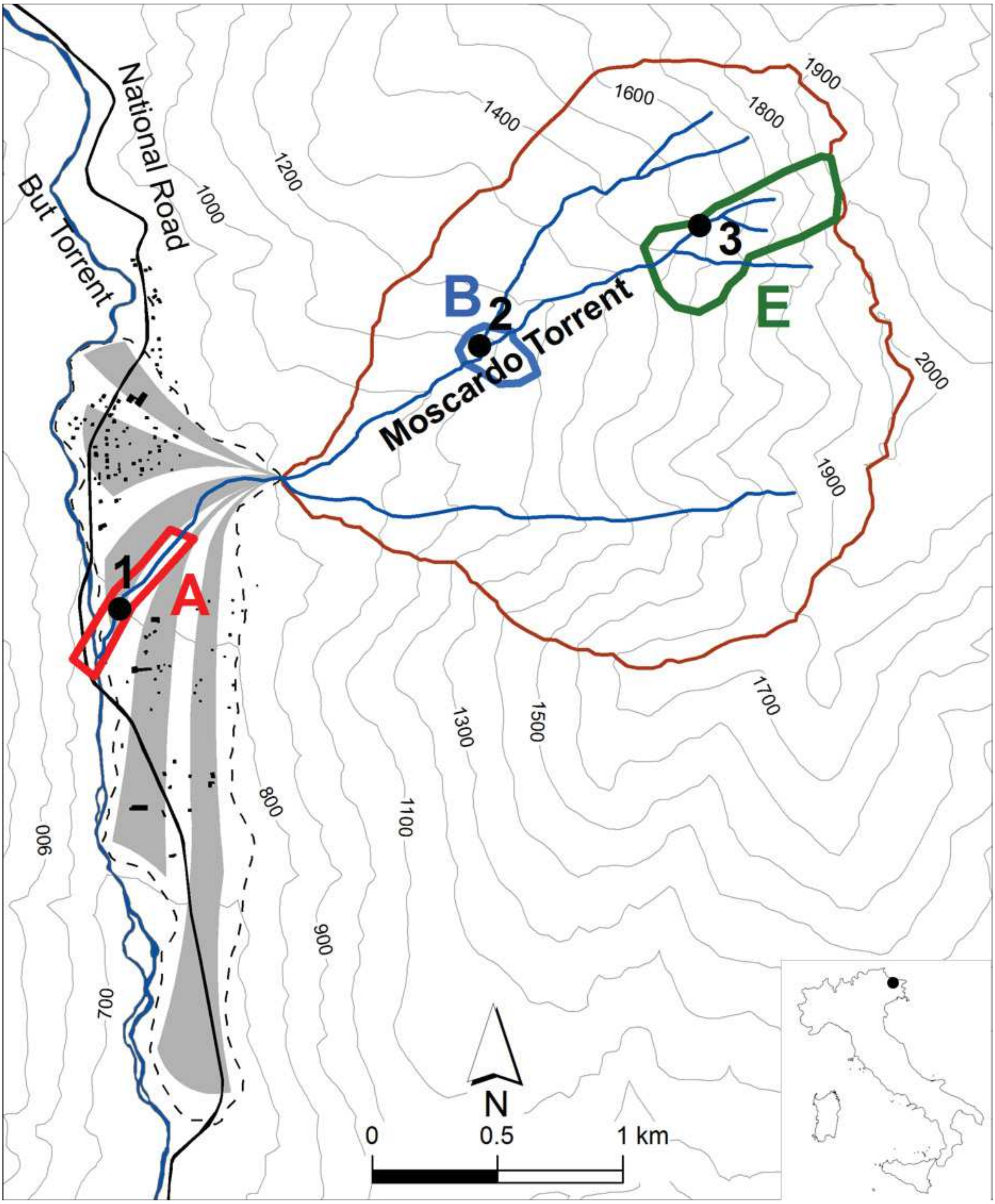

Figure 8-2: Location map of the Moscardo Torrent basin. (1) Instrumented channel stretch; (2 and 3) rain gauges; (A, B, E) TLS surveyed areas

Table 8-1: Summary of study area characteristics

Name	Gadria and Strimm catchments	Moscardo Torrent
Country/Region/Province	Autonomous Province of Bozen-Bolzano (Italy)	Friuli Venezia Giulia Region (Italy)
Drainage area (km²)	14.8 (6.3 km² Gadria, 8.5 km² Strimm)	4.1
Main river basin	Adige River	But and Tagliamento River
Range of elevation (m)	1394 – 3197	890-2043
Geology (dominant rocks)	Metamorphic rocks including para- and ortogneiss, pegmatite	Sedimentary rocks (Flysch)
Quaternary legacy	Glaciated	Glaciated
Human impact	Presence of several check dams in the Gadria creek and of an open check dam with a retention basin at the confluence of Gadria and Strimm creeks	Presence of several check dams along the main channel
Mean annual discharge (m³/s)	n.a.	n.a.
Q10 and Q100 (m³/s)	n.a.	n.a.
Mean annual rainfall (mm)	500	500
Timescale of investigation	Years 2005-2011	Scale of single event (August 2011-October 2012)
Investigated components of the sediment cascade	sediment production / sediment transfer / sediment storage	sediment production/ sediment transfer / sediment storage
Investigated hillslope geomorphic processes	landslide / debris flow	landslide / debris flow
Fluvial sediment transport	n.a.	n.a.

8.1.3 Methods

For assessing geomorphic changes and estimating erosion and deposition volumes, a method based on fuzzy logic developed by Wheaton et al. (2010), was used to derive the DoD maps of both study areas. This method takes into account DEM uncertainties in a spatially variable manner making possible to discriminate real changes from noise. According to Wheaton et al. (2010), the process of accounting for DoD uncertainty requires three main steps consisting of (i) quantifying the uncertainty in the individual DEM surfaces, (ii) propagating the identified uncertainties into the DoD, and (iii) assessing the significance of propagated uncertainty.

The spatially variable uncertainty assessment has been addressed by creating ad-hoc Fuzzy Inference Systems (FIS) (Wheaton et al., 2010) using in inputs geomorphometric parameters as proxy of vertical uncertainty in the DTM: slope and point density in the Gadria-Strimm catchments and slope, point density and Vegetation Noise in the Moscardo catchment. Vegetation Noise is an indicator, recently developed by Blasone et al. (2014), based on the characteristic noise-structures caused by vegetation cover in LiDAR-derived DTMs. It is intended to measure the relative vegetation presence in relation to ground points used for DTM interpolation.

After defining membership functions (MFs) (the process identifying both linguistic adjectives to characterize the variable to be described and the range of values covered by each adjective for inputs and output) on the basis of expert knowledge and the average errors identified in unchanged areas, a map of spatially variable δz (elevation uncertainty) was obtain for each individual DTM.

Following the approach by Brasington et al. (2003) and Lane et al. (2003) based on Taylor (1997) and assuming a normal distribution of errors, individual errors in the DTMs can be propagated into DoD according to the equation:

$$U_{crit} = t\sqrt{(\delta z_{new})^2 + (\delta z_{old})^2} \qquad [1]$$

where Ucrit is the critical threshold error in the DoD or Level of Detection (LoD) of significant elevation change, δznew and δzold are the individual errors in new and old DTM, respectively. Ucrit is based on a critical student’s t-value at a chosen confidence interval where:

$$t = \frac{\left|z_{DEM_{new}} - z_{DEM_{old}}\right|}{\delta u_{DoD}} \qquad [2]$$

where $\left|z_{DEM_{new}} - z_{DEM_{old}}\right|$ is the absolute value of the DoD.

In both study areas, the 95% confidence interval is used as a threshold. For each DoD cell, a critical threshold error is then calculated with Eq. (1) to derive a LoD which is then subtracted from all DoD cells to derive maps of significant elevation change and calculate volumes of erosion and deposition.

To refine DoD uncertainty analysis in the Moscardo catchment, spatial coherence of depositional and erosional units was taken into account. This approach is based on the observation that erosion and deposition tends to occur in spatially coherent patterns (Wheaton et al., 2010) and then DoD predicted elevation changes within those units could have a higher probability of being true.

8.1.4 Results

8.1.4.1 Gadria and Strimm catchments

The topographic changes that occurred from 2005 to 2011 along the channel network of Gadria and Strimm catchments have been assessed. The analysis was based on two high-resolution DTMs (2 m resolution) from airborne LiDAR surveys. DoD map for Gadria and Strimm basins is presented in Figure 8-3. This map is useful to highlight the spatial pattern of geomorphologic changes at basin scale with colors scale ranging from blue (deposition) to red (erosion).

In order to focus on the assessment of geomorphic changes on fluvial and debris flow processes, which is the main objective of the study, a mask that includes channel network and adjacent areas has been created using various informative layers (e.g. hillshade, orthophoto): this has permitted also to exclude areas where inconsistencies between the two DTMs had resulted in unrealistic topographic changes.

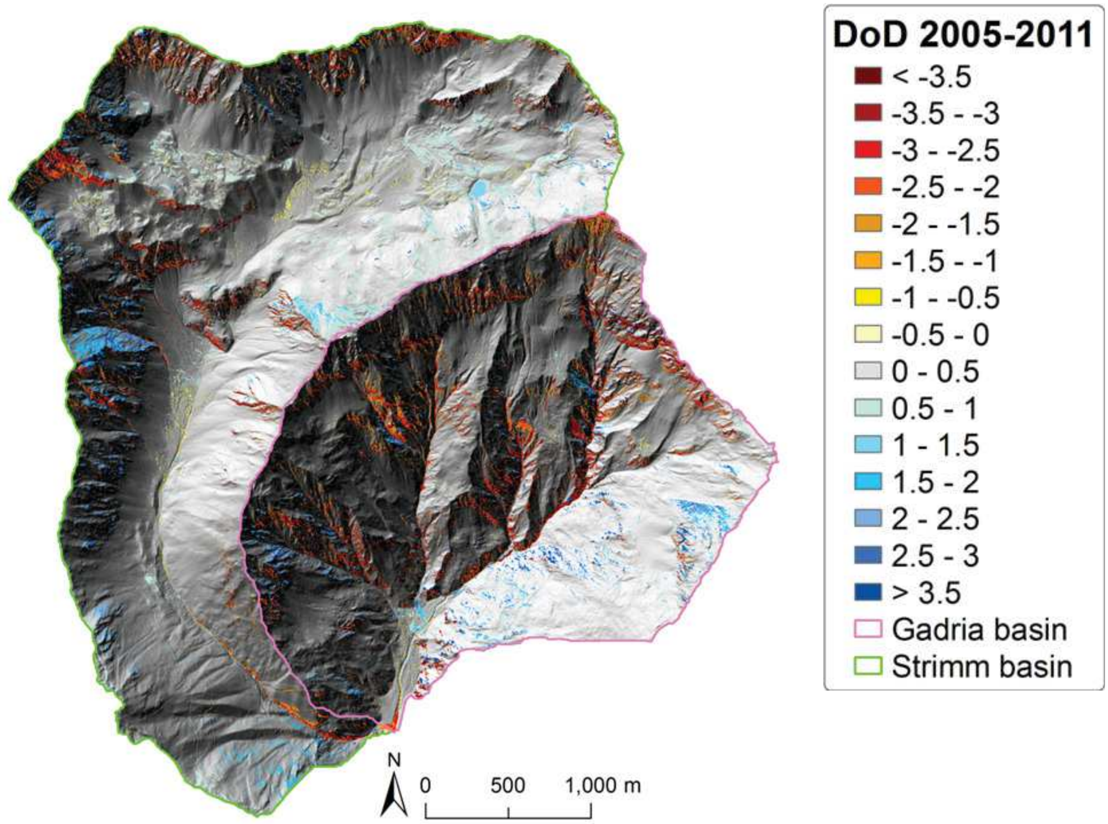

Figure 8-3: DoD map of Gadria and Strimm catchments

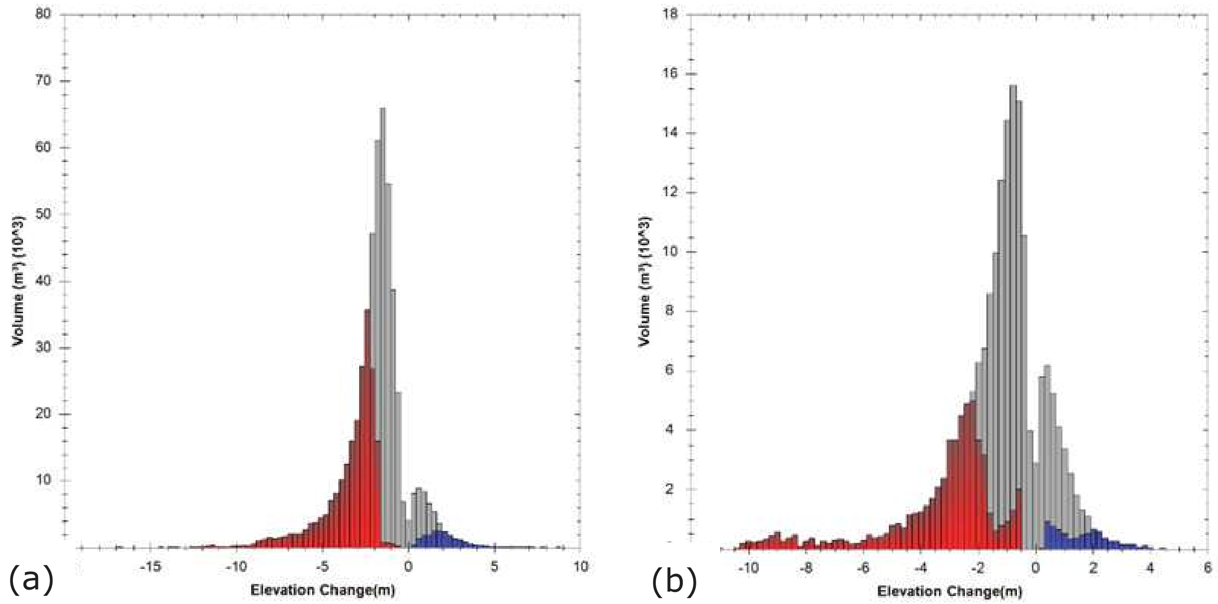

Figure 8-4: Volumetric distributions for Gadria (a) and Strimm (b). Grey shaded areas represent probabilistically thresholded values at 95% confidence interval. Red and blue values represent erosion and deposition respectively.

From areal and volumetric point of view, erosion process dominate in both basins. For the two basins, volumetric elevation change distributions (ECDs) appear to be different (Figure 8-4): ECD of the Gadria shows a very peaked distribution of low magnitude erosion change whereas Strimm ECD is characterized by a bimodal distribution with two peaks of erosion. The peak of relatively high magnitude of erosion is likely due to the main channel near the retention basin, where a debris flow occurred in the summer of 2010. This event was the largest erosion process occurred in the catchment during 2005-2011 time period.

Table 8-2: Volumes calculated with DoD approach compared with historical database for the Gadria catchment

Gadria catchment	*Historical Data Base*	*DoD thresholded*	*Error Volume*
Total erosion (m³)	150,900	198,005	± 86,690
Deposition within the catchment (m³)	16,100	20,955	± 6,909

Table 8-3: Volumes calculated with DoD approach compared with historical database for the Strimm catchment

Strimm catchment	*Historical Data Base*	*DoD thresholded*	*Error Volume*
Total erosion (m³)	35,700	49,791	± 18,872
Deposition within the catchment (m³)	11,700	7,539	± 3,406

Volumes calculated with DoD approach have been then compared with historical database values (Table 8-2 and Table 8-3). To this end, total deposition volumes estimated in the field have been considered as the sediment that remained inside the basin. Conversely, eroded volumes refer to the sediment transported and deposited in the monitored retention basin, located at the confluence of both catchments, from which material is periodically removed. Volumes detected in the field are similar to the ones derived from DoD for both basins. Anyway, it can be observed that DoD results in a volume of total erosion greater than the field estimates of the historical database. In the case of Strimm catchment, this can be partly ascribed to the fact that some events that affected only the upper part of the basin could have remained undetected by field surveys. In general, the comparison between volume estimates of DoD and the historical database are affected by uncertainties in assessing the relative contribution of Gadria and Strimm to sediment deposition in the retention basin at the catchments outlet in the case of events that involved both catchments.

8.1.4.2 Moscardo torrent

Three areas (A, B and E in Figure 8-2) were surveyed using a Riegl LMS-Z620 laser scanner selected for being, for different reasons, exposed to debris-flow dynamics. The downstream area (Area A), is located in the upper part of the alluvial fan, and includes the channel reach monitored with ultrasonic sensors. The second area (Area B) is located in the central part of the basin where a large active roto-translational landslide affects the right bank of the creek (Marcato et al. 2012) and the left bank foot is subjected to erosion. The upstream area (Area E) was chosen for being the main sediment source of the basin.

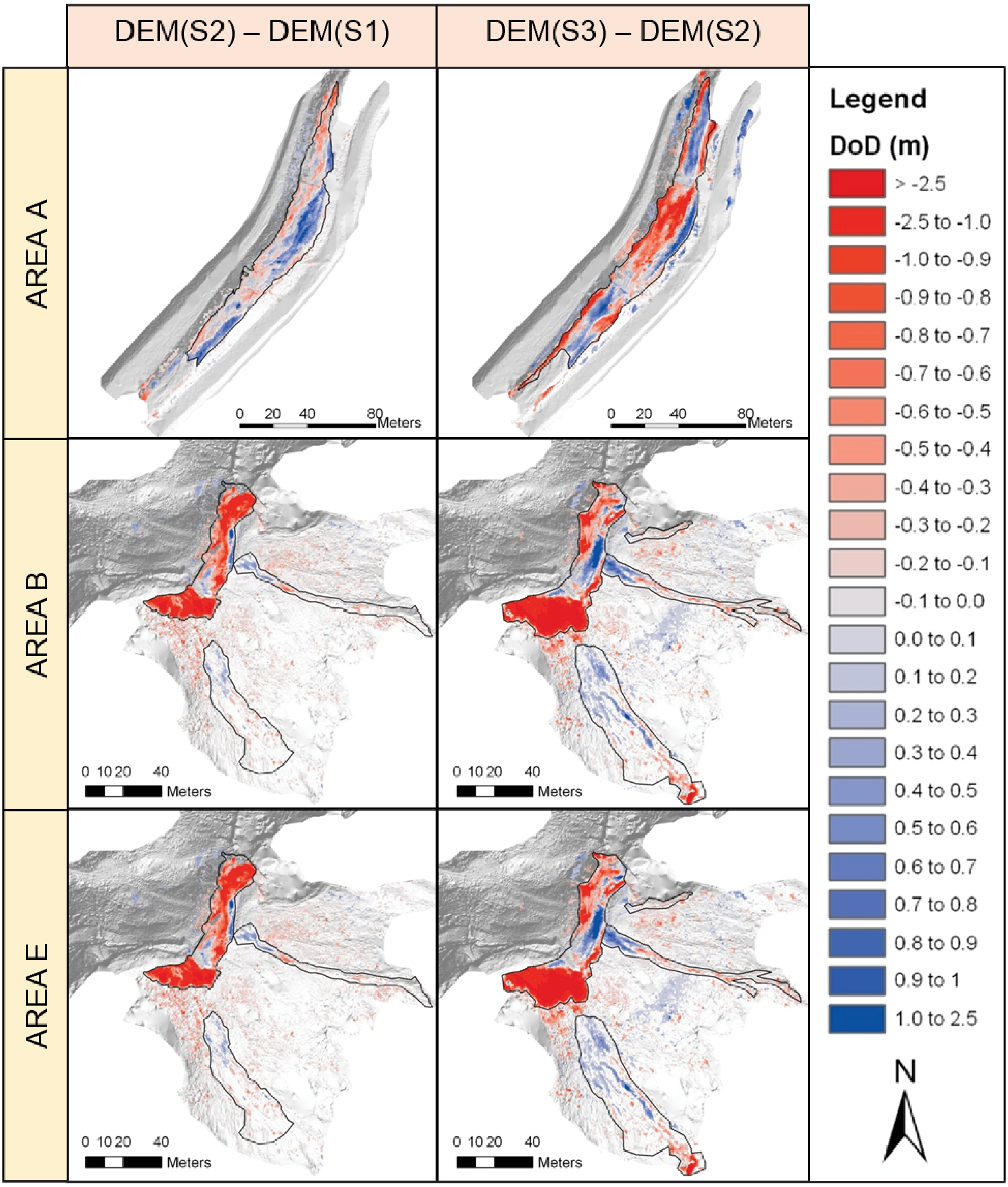

Figure 8-5: DEMs of differences for surveyed areas A, B and E. Left-hand DoDs refer to DEM(S2) – DEM(S1) while right-hand DoDs to DEM(S3) – DEM(S2)

Each area was surveyed three times (referred to, respectively, as S1, S2 and S3), granting the possibility to capture the morphology before and after a debris flow occurred on 14th September 2011 and after two large debris flows recorded on September 24th and 27th of 2012.

Figure 8-5 presents the spatial distribution of differences between subsequent DTMs (0.2 m resolution).

For Area A, the 2011 event involved moderate changes of erosion and deposition, with a prevalence of deposition in the left side of the channel, without particularly affecting the banks. For the 2012 events, more relevant changes can be observed, in particular concerning foot erosion of a large portion of the right side bank.

In Area B, both DoDs show degradation of the channel bed, with foot erosion on the right bank, which, in the 2012 events, led to the removal of riprap that had been built to protect the slope. A 40 meters wide landslide eroded the cliff on the left side, enlarging its area across the events.

For Area E, the pattern of changes is similar between the two DoDs, but the magnitude of the changes in the second DoD, which includes the 2012 debris flows, is higher.

DoD areal and volumetric budgets are summarized in Table 8-4.

Table 8-4: Areal and volumetric DoD results for unthresholded DoDs and for FIS with spatial coherence method. DoD code reported is: area, new survey DEM, old survey DEM (e.g. A21: area A, DoD = DEM(S2) – DEM(S1)).

DoD	Area (m^2)		Volume (m^3)		
	Erosion	Deposition	Erosion	Deposition	Net Change
No uncertainty analysis (unthresholded)					
A21	1399	1330	269	462	+193
A32	2003	1191	1107	480	-627
B21	2256	789	1119	108	-1011
B32	2915	1490	2271	374	-1897
E21	22121	7881	14236	1029	-13207
E32	28697	11152	21004	2033	-18971
Bayesian updating of FIS with spatial coherence (95% CI)					
A21	949	967	244 (±51)	441 (±49)	+198 (±71)
A32	1703	914	1083 (±139)	458 (±87)	-625 (±164)
B21	1290	273	1060 (±83)	80 (±12)	-980 (±84)
B32	1792	817	2162 (±188)	324 (±44)	-1838 (±194)
E21	14449	2221	13723 (±1957)	760 (±170)	-12963 (±1983)
E32	18594	4253	20206 (±2555)	1553 (±378)	-18654 (±2587)

Except from DoD A21 (Area A, DoD = DEM(S2) – DEM(S1)), which shows a modest positive depositional net budget, all DoDs are characterized by negative erosional budgets. Eroded volumes are greater for the 2012 events for all DoDs.

Table 8-5 reports the average erosion/deposition values for surveyed channel and bank areas and channel debris yield rates, which commonly express sediment supply from the channel bed. Area E calculations refer only to the main channel, and do not consider the entire scanned area with secondary channels. These values may be helpful for the geomorphological estimation of volumes, and can be compared with those reported in other studies (e.g., Marchi and D’Agostino, 2004).

Table 8-5: Average erosion/deposition thickness and channel debris yield rate. Values are calculated from Bayesian updating of FIS with spatial coherence (95% CI) results.

DoD	Average erosion/deposition thickness (m)	Debris yield rate (m^3m^{-1})
A21	+0.04 (±0.01)	+1.06 (±0.38)
A32	-0.11 (±0.03)	-3.21 (±0.84)
B21	-0.08 (±0.01)	-11.53 (±0.99)
B32	-0.14 (±0.01)	-21.62 (±2.28)
E21	-0.18 (±0.03)	-13.23 (±2.02)
E32	-0.23 (±0.03)	-12.96 (±1.80)

8.1.5 Conclusions

Compared to airborne LiDAR, the TLS technique is more flexible and accurate in particular for the monitoring of steep areas such as sediment sources in debris-flow catchment. Nevertheless, TLS is limited in terms of range and areal coverage: airborne LiDAR is then a valuable and convenient solution for the monitoring of geomorphic changes at the catchment scale. In order to carry out sound DoD analysis a spatially variable uncertainty assessment is recommended, moreover when using DTMs at different accuracy as in the case of Gadria and Strimm catchments where the 2005 DTM was less accurate than the 2011 DTM. DoD proved to be a very interesting method to rapidly assess geomorphic changes both at catchment scale and in selected sediment sources with a single event time scale. In the case studies, DoD also provides useful information on undetected events within the basins and helps in the identification of erosional and depositional processes in uneasily accessible areas.

10 References related to case studies

Alber, A., Piégay, H., 2011. Spatial disaggregation and aggregation procedures for characterizing fluvial features at the network-scale: Application to the Rhône basin (France). Geomorphology 125, 343-360.

Alfieri, L., Burek, P., Feyen, L., Forzieri, G., 2015. Global warming increases the frequency of river floods in Europe. Hydrol. Earth Syst. Sci. 19, 2247-2260.

Baum, L.E., Eagon, J.A., 1967. An inequality with applications to statistical estimation for probabilistic functions of Markov processes and to a model for ecology. Bull. Amer. Math. Soc., 360-363.

Benda, L., Dunne, T., 1997. Stochastic forcing of sediment supply to channel networks from landsliding and debris flow. Water Resour. Res. 33, 2849-2863.

Bennett, G., Molnar, P., McArdell, B., Schlunegger, F., Burlando, P., 2013. Patterns and controls of sediment production, transfer and yield in the Illgraben. Geomorphology 188, 68-82.

Berger, C., McArdell, B.W., Schlunegger, F., 2011. Sediment transfer patterns at the Illgraben catchment, Switzerland: Implications for the time scales of debris flow activities. Geomorphology 125, 421-432.

Bertrand, M., 2014. Approches régionales de la susceptibilité torrentielle dans les Alpes du Sud. PhD Dissertation, Ecole Normale Supérieure de Lyon, Lyon.

Bertrand, M., Piégay, H., Pont, D., Liébault, F., Sauquet, E., 2013. Sensitivity analysis of environmental changes associated with riverscape evolutions following sediment reintroduction: geomatic approach on the Drôme River network, France. International Journal of River Basin Management 11, 19-32.

Betts, H.D., Trustrum, N.A., Rose, R.C. de, 2003. Geomorphic changes in a complex gully system measured from sequential digital elevation models, and implications for management. Earth Surf. Process. Landforms 28, 1043-1058.

Blasone, G., Cavalli, M., Marchi, L., Cazorzi, F., 2014. Monitoring sediment source areas in a debris-flow catchment using terrestrial laser scanning. Catena 123, 23-36.

Borselli, L., Cassi, P., Torri, D., 2008. Prolegomena to sediment and flow connectivity in the landscape: A GIS and field numerical assessment. Catena 75, 268-277.

Brardinoni, F., Hassan, M.A., Rollerson, T., Maynard, D., 2009. Colluvial sediment dynamics in mountain drainage basins. Earth and Planetary Science Letters 284, 310-319.

Brardinoni, F., Slaymaker, O., Hassan, M.A., 2003. Landslide inventory in a rugged forested watershed: a comparison between air-photo and field survey data. Geomorphology 54, 179-196.

Brasington, J., Langham, J., Rumsby, B., 2003. Methodological sensitivity of morphometric estimates of coarse fluvial sediment transport. Geomorphology 53, 299-316.

Cavalli, M., Trevisani, S., Comiti, F., Marchi, L., 2013. Geomorphometric assessment of spatial sediment connectivity in small Alpine catchments. Geomorphology 188, 31-41.

Cebecauer, T., Hofierka, J., 2008. The consequences of land-cover changes on soil erosion distribution in Slovakia. Geomorphology 98, 187-198.

Chambon, G., Richard, D., Segel, V., 2010. Diagnostic du fonctionnement d’un bassin versant générateur de laves torrentielles et estimation de l’aléa: le cas du Réal (Alpes-Maritimes, France). Sciences Eaux et Territoires, 140-151.

Chen, J., He, Y.P., Wei, F.Q., 2005. Debris flow erosion and deposition in Jiangjia Gully, Yunnan, China. Environ Geol 48, 771-777.

Comiti, F., 2012. How natural are Alpine mountain rivers? Evidence from the Italian Alps. Earth Surf. Process. Landforms 37, 693-707.

Comiti, F., Marchi, L., Macconi, P., Arattano, M., Bertoldi, G., Borga, M., Brardinoni, F., Cavalli, M., d’Agostino, V., Penna, D., Theule, J., 2014. A new monitoring station for debris flows in the European Alps: first observations in the Gadria basin. Nat Hazards 73, 1175-1198.

Cruden, D.M., Varnes, D., 1996. Landslide types and processes. In: Turner, A.K., Schuster, R.L. (Eds.), Landslides. Investigation and mitigation. National Academy Press, Washington, D.C, pp. 36-75.

Derose, R.C., Gomez, B., Marden, M., Trustrum, N.A., 1998. Gully erosion in Mangatu Forest, New Zealand, estimated from digital elevation models. Earth Surf. Process. Landforms 23, 1045-1053.

Desmet, P.J., Govers, G., 1996. A GIS procedure for automatically calculating the USLE LS factor on topographically complex landscape units. Journal of Soil and Water Conservation 51, 427-433.

Feng, X., Wang, Y., Chen, L., Fu, B., Bai, G., 2010. Modeling soil erosion and its response to land-use change in hilly catchments of the Chinese Loess Plateau. Geomorphology 118, 239-248.

Funatsu, K. (Ed.), 2011. New Fundamental Technologies in Data Mining. INTECH.

Gavrilovic, S., 1970. Savremeni načini proračunavanja bujičnih nanosa i izrada karata erozije. Posvet Erozija, bujični tokovi i rečni nanos, Belgrade.

Ghimire, S.K., Higaki, D., Bhattarai, T.P., 2006. Gully erosion in the Siwalik Hills, Nepal: estimation of sediment production from active ephemeral gullies. Earth Surf. Process. Landforms 31, 155-165.

Gomez, B., Banbury, K., Marden, M., Trustrum, N.A., Peacock, D.H., Hoskin, P.J., 2003. Gully erosion and sediment production: Te Weraroa Stream, New Zealand. Water Resour. Res. 39, n/a.

Haas, F., 2008. Fluviale Hangprozesse in Alpinen Einzugsgebieten der Nördlichen Kalkalpen. Quantifizierung und Modellierungsansätze. Profil-Verl., München/Wien.

Haas, F., Heckmann, T., Wichmann, V., Becht, M., 2011. Quantification and Modeling of Fluvial Bedload Discharge from Hillslope Channels in two Alpine Catchments (Bavarian Alps, Germany). Z. Geomorph. N.F. Suppl. 55, 147-168.

Habler, G., Thöni, M., Grasemann, B., 2009. Cretaceous metamorphism in the Austroalpine Matsch Unit (Eastern Alps): The interrelation between deformation and chemical equilibration processes. Miner Petrol 97, 149-171.

Haeberli, W., 1985. Creep of mountain permafrost: internal structure and flow of alpine rock glaciers, Zürich.

Hinderer, M., Kastowski, M., Kamelger, A., Bartolini, C., Schlunegger, F., 2013. River loads and modern denudation of the Alps — A review. Earth-Science Reviews 118, 11-44.

Hubert, P., 2000. The segmentation procedure as a tool for discrete modelling of hydrometeorological regimes. Stochastic Environmental Research and Risk Assessment 14, 297-304.

Lallias-Tacon, S., 2014. in prep. PhD Dissertation, Université de Lyon, Lyon.

Lane, S.N., Westaway, R.M., Murray Hicks, D., 2003. Estimation of erosion and deposition volumes in a large, gravel-bed, braided river using synoptic remote sensing. Earth Surf. Process. Landforms 28, 249-271.

Leviandier, T., Alber, A., Le Ber, F., Piégay, H., 2012. Comparison of statistical algorithms for detecting homogeneous river reaches along a longitudinal continuum. Geomorphology 138, 130-144.

LFU (Ed.), 2014. EGAR-Kartierung: Erläuterungen und Beschreibung der Vegetations- bzw. Hydrotop-Typen in Wildbacheinzugsgebieten. Erläuterungen und Beschreibung der Vegetations- bzw. Hydrotop-Typen in Wildbacheinzugsgebieten, Augsburg.

Liébault, F., Gomez, B., Page, M., Marden, M., Peacock, D., Richard, D., Trotter, C.M., 2005. Land-use change, sediment production and channel response in upland regions. River Res. Applic. 21, 739-756.

Liébault, F., Lallias-Tacon, S., Cassel, M., Talaska, N., 2013. Long profile responses of alpine braided rivers in SE France. River Res. Applic. 29, 1253-1266.

Loye, A., 2013. Budgeting rockfall and modeling sediment delivery in torrent systems. PhD Dissertation, Université de Lausanne, Lausanne.

Mao, L., Cavalli, M., Comiti, F., Marchi, L., Lenzi, M.A., Arattano, M., 2009. Sediment transfer processes in two Alpine catchments of contrasting morphological settings. J. Hydr. 364, 88-98.

Marcato, G., Mantovani, M., Pasuto, A., Zabuski, L., Borgatti, L., 2012. Monitoring, numerical modelling and hazard mitigation of the Moscardo landslide (Eastern Italian Alps). Engineering Geology 128, 95-107.

Marchi, L., Arattano, M., Deganutti, A.M., 2002. Ten years of debris-flow monitoring in the Moscardo Torrent (Italian Alps). Geomorphology 46, 1-17.

Marchi, L., d’Agostino, V., 2004. Estimation of debris-flow magnitude in the Eastern Italian Alps. Earth Surf. Process. Landforms 29, 207-220.

Mari, J.-F., Le, F., Ghali, E., Benot, M., Eng, C., Thibessard, A., Leblo, P., 2011. Using Markov Models to Mine Temporal and Spatial Data. In: Funatsu, K. (Ed.), New Fundamental Technologies in Data Mining. INTECH.

Mathys, N. (Ed.), 1999. Les bassins versants expérimentaux de Draix. Laboratoire d'étude de l'érosion en montagne : séminaire, Draix-Le Brusquet-Digne, 22-24 octobre 1997. CEMAGREF, Grenoble.

Mathys, N., Brochot, S., Meunier, M., Richard, D., 2003. Erosion quantification in the small marly experimental catchments of Draix (Alpes de Haute Provence, France). Calibration of the ETC rainfall–runoff–erosion model. Catena 50, 527-548.

Milan, D.J., Heritage, G.L., Large, A.R., Fuller, I.C., 2011. Filtering spatial error from DEMs: Implications for morphological change estimation. Geomorphology 125, 160-171.

Moore, I., Grayson, R., Ladson, A., 1991. Digital terrain modelling: A review of hydrological, geomorphological, and biological applications. Hydrol. Process. 5, 3-30.

Mosley, M.P., 1980. Mapping sediment sources in a New Zealand Mountain Watershed. Geo 3, 85-95.

Nadal-Romero, E., Martinez-Murillo, J.F., Vanmaercke, M., Poesen, J., 2011. Scale-dependency of sediment yield from badland areas in Mediterranean environments. Progress in Physical Geography 35, 297-332.

Navratil, O., Evrard, O., Esteves, M., Legout, C., Ayrault, S., Némery, J., Mate-Marin, A., Ahmadi, M., Lefèvre, I., Poirel, A., Bonté, P., 2012. Temporal variability of suspended sediment sources in an alpine catchment combining river/rainfall monitoring and sediment fingerprinting. Earth Surf. Process. Landforms 37, 828-846.

Navratil, O., Liébault, F., Bellot, H., Travaglini, E., Theule, J., Chambon, G., Laigle, D., 2013. High-frequency monitoring of debris-flow propagation along the Réal Torrent, Southern French Prealps. Geomorphology.

Neugirg, F., Kaiser, A., Schmidt, J., Becht, M., Haas, F., 2014. Quantification, analysis and modeling of soil erosion on steep slopes using LiDAR and UAV photographs. In: Xu, Y.J. (Ed.), Sediment Dynamics from the Summit to the Sea. IAHS Press, pp. 51-58.

Passalacqua, O., 2013. Utilisation de données LiDAR aéroporté pour l'étude de l'érosion torrentielle : l'exemple du vallon du Réal dans les Alpes-Maritimes. MSc Thesis, Université Joseph Fourier, Grenoble.

Petan, S., 2010. Measurements and spatial modelling of rainfall erosivity of a soil erosion factor. (in Slovenian). PhD Dissertation, University of Ljubljana, Ljubljana.

Petkovšek, G., 2002. Quantification and modelling soil erosion with an spplication on the Dragonja watershed. (in Slovenian). PhD Dissertation, University of Ljubljana, Ljubljana.

Piégay, H., Alber, A., Slater, L., Bourdin, L., 2009. Census and typology of braided rivers in the French Alps. Aquat. Sci. 71, 371-388.

Ranzi, R., Le, T.H., Rulli, M.C., 2012. A RUSLE approach to model suspended sediment load in the Lo river (Vietnam): Effects of reservoirs and land use changes. Journal of Hydrology 422-423, 17-29.

Renard, K.G., Foster, G.R., Weesies, G.A., McCool, D.K., Yoder, D.C., 1997. Predicting soil erosion by water: a guide to conservation planning with the Revised Universal Soil Loss Equation (RUSLE). Agriculture handbook 703.

Sass, O., Haas, F., Schimmer, C., Heel, M., Bremer, M., Stöger, F., Wetzel, K.-F., 2012. Impact of forest fires on geomorphic processes in the Tyrolean Limestone Alps. Geografiska Annaler: Series A, Physical Geography 94, 117-133.

Schlunegger, F., Badoux, A., McArdell, B.W., Gwerder, C., Schnydrig, D., Rieke-Zapp, D., Molnar, P., 2009. Limits of sediment transfer in an alpine debris-flow catchment, Illgraben, Switzerland. Quaternary Science Reviews 28, 1097-1105.

Scotti, R., Brardinoni, F., Alberti, S., Frattini, P., Crosta, G.B., 2013. A regional inventory of rock glaciers and protalus ramparts in the central Italian Alps. Geomorphology 186, 136-149.

Streutker, D.R., Glenn, N.F., Shrestha, R., 2011. ASlope-based Method for Matching Elevation Surfaces. Photogrammetric Engineering and Remote Sensing (Photogram Eng Rem Sensing) 77, 743-750.

Surian, N., Rinaldi, M., 2003. Morphological response to river engineering and management in alluvial channels in Italy. Geomorphology 50, 307-326.

Taillefumier, F., Piégay, H., 2003. Contemporary land use changes in prealpine Mediterranean mountains: a multivariate GIS-based approach applied to two municipalities in the Southern French Prealps. Catena 51, 267-296.

Taylor, J.R., 1997. An introduction to error analysis. The study of uncertainties in physical measurements. University Science Books, Sausalito, Calif.

Theule, J.I., Liébault, F., Loye, A., Laigle, D., Jaboyedoff, M., 2012. Sediment budget monitoring of debris-flow and bedload transport in the Manival Torrent, SE France. Nat. Hazards Earth Syst. Sci. 12, 731-749.

Turner, A.K., Schuster, R.L. (Eds.), 1996. Landslides. Investigation and mitigation. National Academy Press, Washington, D.C.

Vallauri, D., Vincent, P., 1999. Histoire de l'occupation de l'espace au XIXème siècle dans les bassins expérimentaux du Saignon, du Brusquet et du Laval (Alpes-de-Haute-Provence). In: Mathys, N. (Ed.), Les bassins versants expérimentaux de Draix. Laboratoire d'étude de l'érosion en montagne : séminaire, Draix-Le Brusquet-Digne, 22-24 octobre 1997. CEMAGREF, Grenoble, pp. 263-277.

van der Knijf, J., Jones, R., Montanarella, L., 2000. Soil erosion risk assessment in Europe.

van Oost, K., Govers, G., Desmet, P., 2000. Evaluating the effects of changes in landscape structure on soil erosion by water and tillage. Landscape Ecology 15, 577-589.

van Rompaey, A.J.J., Verstraeten, G., van Oost, K., Govers, G., Poesen, J., 2001. Modelling mean annual sediment yield using a distributed approach. Earth Surf. Process. Landforms 26, 1221-1236.

Verstraeten, G., Oost, K., Rompaey, A., Poesen, J., Govers, G., 2002. Evaluating an integrated approach to catchment management to reduce soil loss and sediment pollution through modelling. Soil Use and Management 18, 386-394.

Verstraeten, G., Prosser, I.P., 2008. Modelling the impact of land-use change and farm dam construction on hillslope sediment delivery to rivers at the regional scale. Geomorphology 98, 199-212.

Wheaton, J.M., Brasington, J., Darby, S.E., Sear, D.A., 2010. Accounting for uncertainty in DEMs from repeat topographic surveys: improved sediment budgets. Earth Surf. Process. Landforms 35, 136-156.

Xu, Y.J. (Ed.), 2014. Sediment Dynamics from the Summit to the Sea. IAHS Press.